PHYSICAL REVIEW B

CONDENSED MATTER

THIRD SERIES, VOLUME 39, NUMBER 2 15 JANUARY 1989-I

Temperature dependence and anharmonicity of the Debye-Waller factor in sodium metal using Mössbauer γ-ray diffraction

M. L. Crow,* G. Schupp, and W. B. Yelon
Research Reactor and Department of Physics and Astronomy, University of Missouri, Columbia, Missouri 65211

J. G. Mullen and A. Djedid
Department of Physics, Purdue University, West Lafayette, Indiana 47907
(Received 25 April 1988)

The Debye-Waller factor of sodium has been measured as a function of temperature from 80 to 295 K using Mössbauer γ-ray scattering. The high energy resolution provided by this technique allowed experimental separation of the elastic scattering from the inelastic thermal diffuse scattering. The results were compared with the harmonic model using integrations over dispersion curves from the neutron-scattering measurements of Woods *et al.* and the lattice-dynamics calculations of Glyde and Taylor. The Debye-Waller exponent was shown to exceed the harmonic prediction by 23% at room temperature. This difference is attributed to anharmonic terms in the interatomic potential.

INTRODUCTION

The reduction of the elastic Bragg scattering by the thermal motion, characterized by the Debye-Waller factor, is a measure of the lattice-dynamical properties of a crystal. Its strong dependence on temperature provides a method of understanding the magnitude of anharmonic terms in lattice dynamics. The measurement of the Debye-Waller factor is complicated, however, by the thermal diffuse scattering (TDS), which is inelastic scattering due to lattice excitations. Although both effects are due entirely to lattice vibrations, detailed modeling is necessary to extract a complete picture or even a reliable estimate of the size of the inelastic contribution[1] for x-ray or neutron scattering. Mössbauer γ-ray scattering provides a method of experimentally separating the elastic and inelastic scattering, since the Mössbauer linewidth is typically less than 1 μeV. The separation technique can be used to examine the momentum space dependence of the TDS, or to measure the temperature factor independent of the TDS. This technique has been applied to a study of the temperature dependence of the Debye-Waller factor in Na from 80 to 295 K. The TDS-free Debye-Waller factor was compared with phonon dispersion relations obtained from neutron diffraction and lattice-dynamics calculations[2,3] to determine the size of the anharmonic terms.

EXPERIMENTAL PROCEDURES

The Mössbauer diffraction instrument at the University of Missouri Research Reactor (MURR) has been described in detail by Yelon *et al.*[4] The present experiments utilize the 46.48-keV transition in ^{183}W, which has an energy width of 4.8 μeV. Irradiation of ^{181}Ta foils in a 2.5×10^{14} neutrons/cm^2 s flux at MURR for one week produces 70-Ci sources of 5.1-d ^{183}Ta. The shielding assembly contains a liquid-nitrogen cryostat, which allows the source to be cooled in order to enhance the recoilless emission fraction. For the Na experiments described herein, a LiF(200) monochromating filter was used to select the 46.48-keV γ rays from the complex source spectrum to minimize background. A Soller collimator was placed between the monochromating filter and the sample to restrict the vertical divergence (perpendicular to the scattering plane) of the incident beam. This restriction had two effects: the reduced vertical divergence of the incident beam gave improved momentum resolution in the vertical direction, while the height reduction allowed the detector to accept the full vertical divergence of the scattered beam at all scattering angles. The sample stage was automated to move in the scattering plane, and the scattering angle was adjusted by moving the detector and absorber assembly. Four 96% enriched ^{183}W absorbers were mounted in a "paddle-wheel" rotor, which could be driven at speeds varying from 0.5 to 300 cm/s. An intrinsic Ge detector provided nearly complete separation of the 46.48-keV γ rays from other peaks in the γ-ray spectrum.

The procedure for separating the elastic and inelastic scattering used the on-off resonance method, which was described in detail in our earlier work on Si.[5] This method consists of counting the scattered γ rays at two rotor velocities. The "on" resonance velocity of 0.64

cm/s was well within the linewidth, and the "off" resonance velocity of 19.2 cm/s was much larger than the linewidth. The elastic intensity can be determined from the difference between these two count rates, and the inelastic intensity can be inferred by comparing the elastic intensity with the total high-velocity intensity. The resonance parameters were determined for each freshly irradiated source by measuring the velocity spectrum for the radiation reflected from a LiF crystal set at the (200) Bragg peak. The LiF reflections have been demonstrated to be essentially 100% elastic.[6] The resulting intensities were fit to a Lorentzian representation of the Mössbauer line shape, using a least-squares method. In light of our recent work on Mössbauer line-shape analyses,[7] it must be noted that the on-off resonance method using a Lorentzian line shape is a simplifying approximation that must be justified. Analyses with the correct line shape showed that the on-resonance minima were consistently $0.73\pm0.04\%$ shallower than those given by the Lorentzian line shape for all the sources used. Since the measurements of the elastic intensities for the Bragg peaks studied here essentially depended only on relative counting rates, this difference did not affect the final result. The principal reason for the consistency was the fact that resonance data were all collected over the same velocity range of approximately ±20 linewidths. Since the Lorentzian shape does not approach the off-resonance continuum in the correct asymptotic limit, a smaller velocity range would lead to a larger (but still proportional) effect; but more importantly, different velocity ranges would lead to inconsistent results. Taking the resonance dip to be proportional to the recoilless fraction is itself an approximation, but in our case where the absorber temperature is constant, it is simply a multiplicative constant. Although it was not significant in these measurements, changes in the recoilless fraction due to source resonance self-absorption can also be a complicating effect.

The sample in this experiment was an approximately cylindrical Na single crystal about 2.5 cm in diameter and 5.5 cm high, encased in an Al sample can. The crystal was grown by S. A. Werner.[8] The crystal was oriented in a (001) plane with the cylinder axis inclined about 23° from the vertical direction. For low-temperature measurements, the sample was mounted in a gas-flow cryostat using liquid nitrogen as the cooling medium. The temperature was measured and controlled with a germanium diode sensor. Room-temperature measurements were performed with the sample outside the cryostat.

Series of Bragg reflections in the $(hh0)$ and $(h00)$ directions were measured using the on-off resonance method, at 80, 130, 160, 205, and 295 K. The change in scattering angles as a function of temperature was consistent with thermal expansion data.[9] In order to characterize the position and mosaic structure of each reflection, a detailed off-resonance omega rocking curve was obtained for comparison with each omega on-off scan. Figure 1 shows a typical omega scan for a (110) reflection, and Fig. 2 shows an omega scan for a (200) reflection. In order to obtain reliable integrated intensities from the limited number of steps used in the on-off

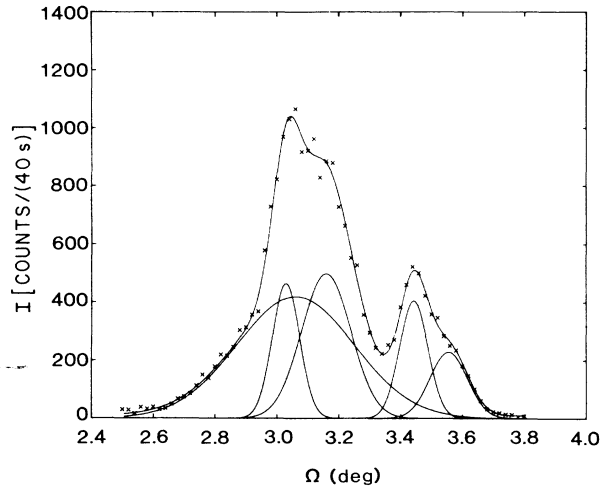

FIG. 1. Rocking curve for the (110) Bragg reflection from the Na crystal. The smooth curve is a fit parametrized by five Gaussians and a small continuum.

scans (usually five position settings for each Bragg peak), some method of accounting for the irregularity in the mosaic structure was required. The method used was to parametrize the shape of the rocking curves using a set of Gaussian profiles, with parameters selected by a least-squares fitting method. The appropriate number of Gaussian profiles for each direction was selected by adding Gaussians until the χ^2 value no longer improved; the (110) profile shown in Fig. 1, for example, was parametrized by five Gaussians and a constant continuum. It was notable that for each of the two series of reflections the rocking curves were characterized by a series of Gaussians of approximately constant width and

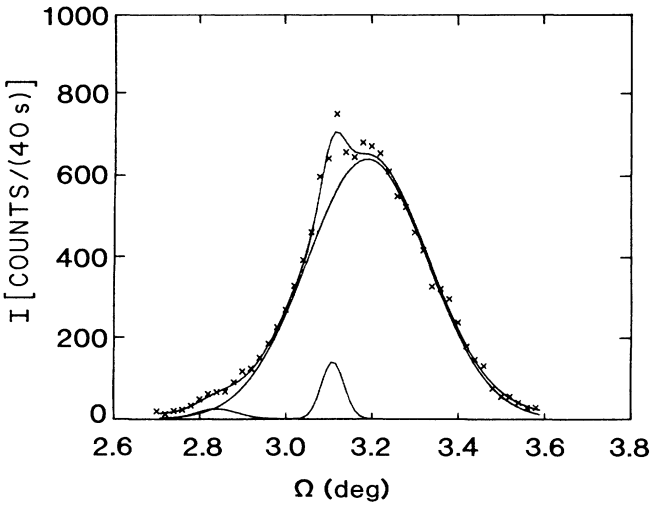

FIG. 2. Rocking curve for the (200) Bragg reflection from the Na crystal. The smooth curve is a fit parametrized by three Gaussians and a small continuum.

relative position, but of varying relative height. The most probable explanation for the observed variation in the rocking curves is that the crystal has a number of large, relatively perfect grains which contribute to the profile; the height variation is presumably due to small changes in the set of grain volumes of the crystal illuminated as the scattering angle was changed. Once the shape of the rocking curve was parametrized, the elastic data were fit to the same shape, and an integrated intensity was determined. The accuracy of the area determinations was checked by performing fits with differing starting parameters; the variation in the resulting areas was far smaller than the expected error from counting statistics.

The size of the inelastic contribution increased with Q^2, where Q was the total momentum transfer with magnitude $|\mathbf{Q}|=4\pi\sin\theta/\lambda$, and with temperature. The inelastic contribution was significant for every reflection measured except for the (110). For some high-angle reflections, such as the (440) at 80 K and the (330) at 295 K, it was as large or larger than the integrated elastic intensity.

The data were collected with a series of different sources, so that it was necessary to normalize the intensities. When each freshly irradiated source was transferred to the instrument, a series of alignment procedures was performed, and a LiF crystal was mounted and oriented as a standard for the recoiless fraction determination. Since the same crystal in nearly the same orientation was used each week, the observed intensity also served as a measure of relative source intensity. Rocking curves in ω and $\theta-2\theta$ were collected to verify the LiF orientation. Attenuation by the cryostat was measured by direct beam absorption to be 0.70, in agreement with absorption tables. Since the on-off measurements were dependent on the recoilless fractions, the relative recoilless fractions were included in the normalization factors.

ANALYSES

The intensity of an allowed elastic Bragg reflection in sodium is given by

$$I=f^2(\mathbf{Q})\frac{1+\cos^2(2\theta)}{2\sin(2\theta)}\exp(-2W)\ , \tag{1}$$

where $f(\mathbf{Q})$ is the atomic scattering factor for sodium, 2θ is the scattering angle, and W is the temperature factor. The observed elastic intensities were divided by f^2 and by the polarization and Lorentz factors, giving numbers which should be dependent only on the temperature factor. Since $2W$ is proportional to Q^2, a Wilson plot $((\ln I)\{2\sin(2\theta)/f^2[1+\cos^2(2\theta)]\}$ versus $Q^2)$ is expected to be a straight line. Corrections to Eq. (1) due to the slight polarization caused by the monochromating filter were less than 0.1% and were not included.

Figure 3 is a Wilson plot using the normalized intensity values. The initial attempt to analyze the data was to fit all of the intensities at each temperature to a straight line. Two systematic features were indicated by this procedure. First, the (110) reflection was very low in intensity for each temperature, in some cases even lower than the (200). In an attempt to understand the reduction of

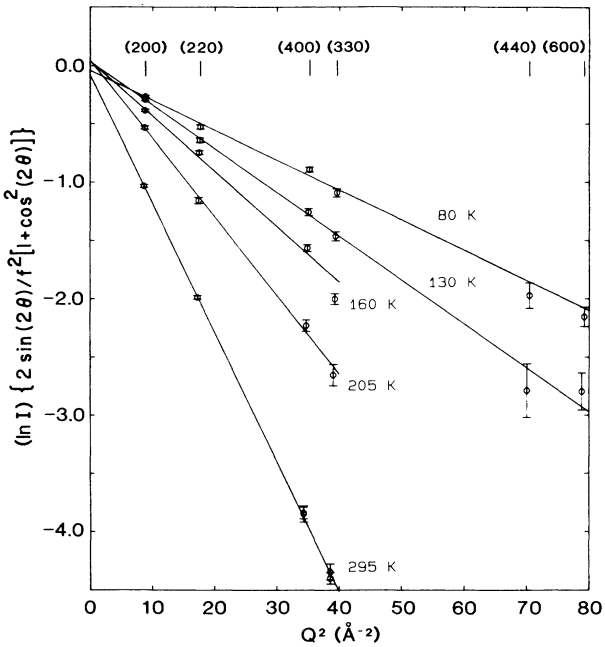

FIG. 3. Wilson plot with normalized values of $(\ln I)\{2\sin(2\theta/f^2[1+\cos^2(2\theta)]\}$ for the different temperatures indicated in the figure. The particular Bragg reflection represented by each data point is given along the top of the figure.

the (110) intensity, the relative intensities of the (110) and (220) reflections were measured using 0.12-Å γ rays and 1.06-Å neutrons, which produced similar results. The most probable explanation is that the Na crystal contained several large, perfect grains, as indicated by the rocking curves, and that extinction was a large effect in the (110) reflection. The extinction apparently did not affect the (200), which had smaller scattering and Debye-Waller factors. The (110) data were excluded from further analyses.

Secondly, when the unnormalized $(h00)$ and $(hh0)$ data were graphed on independent Wilson plots, the $\ln I$ intercepts for the same temperature were different. The points in the $(h00)$ and the $(hh0)$ directions were then fit separately to straight lines for each temperature using a least-squares method, with and without the (110) data included. When the (110) data were excluded, the fits to the two directions gave nearly equal slopes, and the difference between the $(hh0)$ and $(h00)$ intercepts was independent of temperature, with the $(h00)$ intensity about 24% lower. The difference in intensities between the $(hh0)$ and $(h00)$ directions was probably due to a combination of crystal volume and absorption effects. The substantial difference in the mosaic structure in the two directions indicates that distinct volumes were being sampled. The absorption was measured by rotating the crystal through 65°, covering the range of the measurements, and measuring the transmission of γ rays with the detector at the zero position. This measurement indicates an increase in absorption of about 9% when the crystal was rotated by 45°, which corresponds to the difference in orientation between the $(hh0)$ and $(h00)$ series, indicat-

TABLE I. Debye-Waller slopes (in Å^2) predicted by integrations using the Glyde and Taylor frequency spectrum at 5 K, frequency spectra as a function of temperature, and determined experimentally.

T (K)	Integration with 5-K frequencies	Integration with frequency temperature dependence	Experimental slopes
80	−0.0235	−0.0238	−0.0257(11)
130	−0.0361	−0.0370	−0.0376(17)
160	−0.0438	−0.0453	−0.0474(12)
205	−0.0556	−0.0594	−0.0674(17)
295	−0.0794	−0.0902	−0.1108(15)

ing that less than half of the intensity difference were due to absorption. All of the $(hh0)$ data were subsequently normalized with respect to the $(h00)$ data by multiplying by a factor of 0.76, and combined with them to give Fig. 3.

During the fitting process, an effort was made to determine whether a Q^4 dependence could be measured, as was reported for lithium.[10] The data did not indicate the presence of a statistically significant Q^4 term at any of the temperatures measured. The remaining analyses were carried out in terms of the clearly measurable Q^2 dependence.

To check the consistency of the data, the overall Wilson-plot slopes for each temperature were obtained by two methods. In one method the slopes determined independently for the $(hh0)$ and $(h00)$ directions were averaged. In the other, the $(h00)$ intensities were first multiplied by the average scaling factor of 1.24 determined from the intercepts and then a linear fit was performed on the combined data. These two methods agreed within 0.5% except for the 160-K slope. The discrepancy at this temperature can be accounted for by the small number of points. The last column of Table I lists the experimental slopes obtained for each temperature.

DETERMINATION OF HARMONIC SLOPES

The slopes determined experimentally in this investigation represent the total Debye-Waller factor as a function of temperature. To get the size of the anharmonic contribution, it is necessary to calculate the harmonic contribution, which can be done if the frequency spectrum is known. For sodium, the low-temperature dispersion curves are well known,[2] and data on the temperature dependence are available.[3] Once the magnitude of the harmonic contribution has been determined, the magnitude and temperature dependence of the anharmonic contributions can be examined and compared with existing models.

The Debye-Waller factor $2W_n$ for a single atom is defined by

$$\exp(-2W_n)=\langle \exp[i\mathbf{Q}\cdot\mathbf{u}_n(t)]\rangle \ , \tag{2}$$

where $\mathbf{Q}$ is the total wave-vector transfer and $\mathbf{u}_n(t)$ is the displacement of atom n. In the harmonic approximation the total Debye-Waller factor can be written

$$\exp(-2W)=\exp\left[-\frac{1}{NM}\sum_{\mathbf{q},j}\frac{[\mathbf{Q}\cdot\mathbf{e}_j(\mathbf{q})]^2}{[\omega_j(\mathbf{q})]^2}E_j(\mathbf{q})\right] , \tag{3}$$

where M is the mass of a sodium atom, N is the number of unit cells in the crystal, $\mathbf{q}$ is the phonon wave vector, and j is the phonon polarization index. The phonon polarization vector is $\mathbf{e}_j(\mathbf{q})$, and the crystal energy associated with phonon state j is $E_j(\mathbf{q})=h\nu_j(\mathbf{q})(\{\exp[\beta h\nu_j(\mathbf{q})]-1\}^{-1}+\frac{1}{2})$. For a cubic crystal, Maradudin *et al.*[11] write

$$\exp(-2W)=\exp\left[-\frac{hQ^2}{12\pi NM}\sum_{\mathbf{q},j}\frac{\coth[\beta h\nu_j(\mathbf{q})/2]}{2\pi\nu_j(\mathbf{q})}\right] . \tag{4}$$

In both of these equations, the sum on $\mathbf{q}$ is over the first Brillouin zone (BZ). Given an expression for the phonon frequencies $\nu_j(\mathbf{q})$, Eq. (4) can be written as

$$2W=\frac{hQ^2}{12\pi M}\frac{V_{\text{cell}}}{(2\pi)^3}\int_{\text{BZ}}\sum_j\frac{1}{2\pi\nu_j(\mathbf{q})}\coth\left[\frac{h\nu_j(\mathbf{q})}{2k_BT}\right]d^3\mathbf{q} \tag{5}$$

and integrated numerically.

The frequency spectrum of sodium was first studied extensively at 90 K by Woods *et al.*[2] by inelastic neutron scattering. This work produced very detailed phonon dispersion curves, which were interpreted in terms of the harmonic Born–von Karman model. The temperature dependence of the frequency spectrum was investigated by Glyde and Taylor,[3] who calculated dispersion curves using theoretical interatomic potentials, and used the known thermal expansion properties to account for anharmonic effects, at a series of temperatures ranging from 5 to 361 K. These dispersion curves can be described in the Born–von Karman approximation, allowing various frequency integrations to be performed conveniently. Glyde and Taylor give a total of 14 frequency values at each temperature considered, as well as calculated elastic constants. These values were described (for the purpose of integration) at all temperatures using a three-neighbor Born–von Karman model, with seven force constants. It should be noted that the Glyde and Taylor study does not consider the effect of the partial phase transition at 36 K (Ref. 12). A recent neutron-scattering study[13] which concentrated on phonon frequencies near the phase transition agreed for the most part with the Glyde and Taylor results, including the decrease of the $(q,q,0)$ TA_1 mode near the zone boundary with decreasing temperature.

Integrations of Eq. (5) have been performed over the irreducible section of the first Brillouin zone using an Euler-McLaurin summation method. The mesh size chosen for these integrations was much smaller than necessary to make the results independent of the size. The results of these integrations, which first used the 5-K

frequencies at all temperatures and then used frequencies appropriate for the five measured temperatures, are given in Table I along with the experimental Wilson-plot slopes from the on-off resonance measurements. The calculations agree quite well with the data at 80 K, but a gradually increasing difference is apparent at higher temperatures, even when the high-temperature dispersion curves from Glyde and Taylor are used. At room temperature, the observed slope (0.1108 Å^2) is 23±2% greater than the result calculated using room temperature dispersion curves, indicating that the harmonic expression of Eq. (3) is not a complete representation of the Debye-Waller factor.

DISCUSSION

The fundamental assumption in the harmonic approximation is that the variation in the interatomic potential is proportional only to the square of the displacement. A potential is said to be anharmonic if it contains cubic or higher-order terms. The potential for an atom in a cubic crystal with cubic and quartic terms can be written[1]

$$V(u_1,u_2,u_3)=V_0+\tfrac{1}{2}\alpha_0 u^2+\beta_0 u_1u_2u_3+\gamma_0 u^4 +\delta_0(u_1^4+u_2^4+u_3^4-\tfrac{3}{5}u^4)\ , \quad (6)$$

where the strength of the harmonic potential is represented by α_0, β_0 is the cubic anharmonic parameter, and γ_0 and δ_0 are the quartic anharmonic parameters. The displacement of an atom from its equilibrium position is $\mathbf{u}$, and u_1,u_2,u_3 are its Cartesian components. The functional form of the Debye-Waller factor with cubic and quartic anharmonic terms has been examined extensively by Maradudin and Flinn,[14] who write

$$\exp(-2W)=\exp[-(2W_0+2W_1+2W_2+2W_3+2W_4)]\ . \quad (7)$$

The term $2W_0$ is the harmonic part, identical to Eq. (5). The terms $2W_1$ and $2W_2$ are due to the quartic and cubic terms in the potential, respectively, and are both proportional to T^2 and Q^2. The terms $2W_3$ and $2W_4$ are proportional to Q^4 and T^3. As mentioned earlier, the presence of a Q^4 dependence was not evident in our data. Willis[1] showed that $\beta_0=0$ for a cubic monatomic lattice, and that the term in δ_0 is much less than γ_0. Then, the expression for the Debye-Waller slope could be rewritten as

$$\frac{2W}{Q^2}=\frac{2W_h(T)}{Q^2}\left[1+T\left[2\chi\gamma_G-20k_B\frac{\gamma_0}{\alpha_0^2}\right]\right]\ , \quad (8)$$

where $2W_h(T)$ is the harmonic term with no thermal expansion. The product $2\chi\gamma_G$, where χ is the thermal expansion coefficient and γ_G is the Gruneisen parameter, represents the change in the contributions from the frequency spectrum as a function of temperature. The term $20k_B\gamma_0/(\alpha_0^2)T$ is the term in Q^2 due to the quartic term in the potential.

The numerical results and data from Table I were interpreted in terms of Eq. (8) by fitting the slopes to the approximate form

$$\frac{2W}{Q^2}=C_1\left[\frac{1}{\exp[T_{\rm eff}/T]-1}+\frac{1}{2}\right](1+C_{\rm ex}T^2+C_2T)\ ,$$

where C_1 and $T_{\rm eff}$ are parameters describing the sum of the Bose-Einstein distributions for the phonon spectrum. This form was used because the high-temperature limit $E_j(\mathbf{q})=k_BT$, equivalent to neglecting the zero-point motion, is not valid at 80 K. The upper points in Fig. 4 (denoted by x) are the slopes found by integration of the 5-K frequencies listed in Table I. By setting $C_2=0$ and $C_{\rm ex}=0$, a least-squares fit with $C_1=-0.02348$ Å^2 and $T_{\rm eff}=87.86$ K gave the smooth curve shown through the points. The flattening of the slopes at low temperature is a consequence of the zero-point energy. The extremely good fit obtained by our parameters C_1 and $T_{\rm eff}$ in Eq. (9) to the $W_h(T)$ integrations using the 5-K frequencies demonstrates the appropriateness of the approximate form used in Eq. (9). The middle points in Fig. 4 (denoted by +) are the slopes from Table I found by integrating the frequencies appropriate for the different temperatures. The smooth curve through these points used C_1 and $T_{\rm eff}$ from the above fit along with $C_2=0$ to give the best value for $C_{\rm ex}$ of 1.56×10^{-6} K^{-2} to represent the thermal expansion. This representation agrees with specific heat and thermal expansion measurements[9] over the 80–295 K temperature range, as well as with the integrations using the temperature dependent dispersion relations from Glyde and Taylor. C_2 is the parameter describing that part of the anharmonic terms which are linear in T. The lower points on Fig. 4 (with error bars) are the experimental slopes from Table I. With C_1, $T_{\rm eff}$, and $C_{\rm ex}$ fixed at the values determined by the two fits

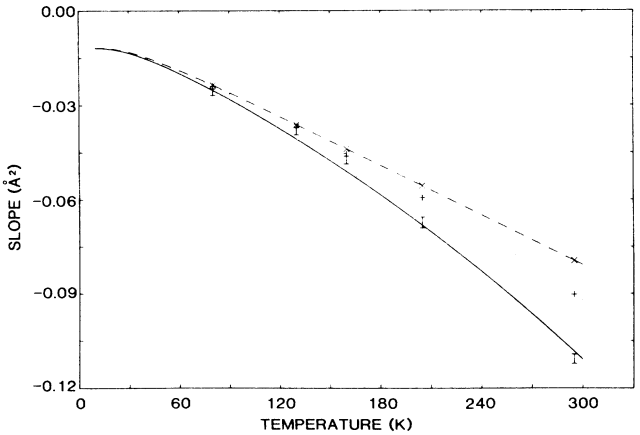

FIG. 4. Experimental slopes determined from the data shown in Fig. 3 plotted vs temperature. Also plotted are the other results from Table I based on the Glyde and Taylor frequency spectra at 5 K (×) and at experimental temperatures (+). The three smooth curves through the calculated and experimental points were obtained by successive fits to Eq. (9) as described in the text.

above, the smooth curve through the data was found by a least-squares fit to C_2 which gave a value of $C_2 = -20k_B\gamma_0/(\alpha_0^2) = 7.789\times10^{-4}$ K^{-1}. At room temperature, this gives values of

$$\alpha_0 = k_B TQ^2/(2W_h) = 5.13\times10^{-13} \text{ erg/Å}^2 ,$$

and therefore $\gamma_0 = -7.42\times10^{-14}$ erg/Å^4. The relative values of γ_0 and α_0 give a measure of the size of the anharmonic potential. The anharmonic contribution represented by the C_2 term at room temperature is 20%.

The discrepancies seen in Fig. 4 between the experimental data and the systematic fit of Eq. (9) indicate a temperature dependence for C_2. Equation (8) does not include a temperature dependence in γ_0, although Willis[1] did suggest a weak temperature dependence. Allowing a linear temperature dependence in the anharmonic term, however, does result in a better fit to the present data. If a term, of the form $C_2(1+C_3T)$, is substituted for C_2 in Eq. (9), values of $C_2 = 1.26\times10^{-6}$ K^{-1} and $C_3 = 2.34$ K^{-1} are obtained by a least-squares fit (where C_1, T_{eff}, and C_{ex} were fixed at the above values). At this stage if only C_{ex} is fixed and the other parameters varied, very similar results are obtained, all with nominal 10% uncertainties. While other fitting procedures can be used, the basic result is that the data are best represented by essentially a linear temperature dependence for γ_0, which is dominated by the C_2C_3 product of 2.95×10^{-6} K^{-2}. This parametrization gives a value of -8.29×10^{-14} erg/Å^4 for γ_0 at room temperature. Since this fit happens to go through the experimental data point at room temperature, it corresponds to the anharmonic contribution of 23±2% noted earlier. Although there is no theoretical prediction for this functional form, the work of Maradudin and Flinn[14] indicates that the anharmonic terms have a much stronger dependence on changes in the frequency spectrum than the quasiharmonic term.

Clearly, the anharmonic effects in Na are far stronger than in the cases examined by Willis[1] (KCl and BaF_2). A comparison to the other alkali metals is somewhat more difficult because few reliable high-temperature Debye-Waller measurements are available. An early x-ray powder diffraction study[15] in Na which made no allowance for TDS obtained a very low room-temperature value for $2W/Q^2$ of 0.0456 Å^2. To simulate the effect of a high-resolution diffraction experiment with no TDS correction, the off-resonance data at 295 K from the present work were analyzed, yielding a value for $2W/Q^2$ of 0.0797 Å^2, which is still smaller than the calculated harmonic factor of 0.0902 Å^2 given in Table I. It is of course possible to correct for the size of the TDS contribution, but the on-off resonance method eliminates the need for this correction.

The present results differ markedly from the inelastic incoherent neutron-scattering measurements on Li, which indicated a large Q^4 term.[10] The magnitude of such a term in Na (at 295 K, where it was expected to be largest) was estimated to be less than 1×10^{-4} Å^4, or at least 4.0 times smaller than the value reported for Li. Maradudin and Flinn[14] show that the Q^4 term includes a mass dependence of M^{-4}, which explains the relatively smaller effect in Na compared to Li.

The Mössbauer scattering technique, in conjunction with measured or calculated dispersion curves, is a relatively direct method for determining the size of anharmonic effects and therefore the strength of anharmonic terms in potentials.

ACKNOWLEDGMENTS

We want to thank Professor S. A. Werner for lending us the Na crystal used in this investigation. We also want to thank Dr. H. R. Glyde for helpful discussions concerning the theoretical calculations. This work was performed with the support of the U.S. Department of Energy, under Grant No. DE-FG02-85ER45200 and No. DE-FG02-85ER45199-A00.

*Present address: Department of Physics, University of Rhode Island, P.O. Box 817, Kingston, RI 02881-0817.

[1]B. T. M. Willis, Acta Crystallogr. A **25**, 277 (1969).
[2]A. D. B. Woods, B. N. Brockhouse, R. H. March, A. T. Stewart, and R. Bowers, Phys. Rev. **128**, 1112 (1962).
[3]H. R. Glyde and R. Taylor, Phys. Rev. B **5**, 1206 (1972).
[4]W. B. Yelon, G. Schupp, M. L. Crow, C. Holmes, and J. G. Mullen, Nucl. Instrum. Meth. B **14**, 341 (1986).
[5]M. L. Crow, G. Schupp, W. B. Yelon, J. G. Mullen, and A. Djedid, Acta Crystallogr. A **43**, 638 (1987).
[6]J. G. Mullen and J. R. Stevenson, in *Workshop on New Directions in Mössbauer Spectroscopy (Argonne, 1977)*, Proceedings of the Workshop on New Directions in Mössbauer Spectroscopy, AIP Conf. Proc. No. 38, edited by G. J. Perlow (AIP, New York, 1977).
[7]J. G. Mullen, A. Djedid, G. Schupp, D. Cowan, Y. Cao, M. L. Crow, and W. B. Yelon, Phys. Rev. B **37**, 3226 (1988).
[8]S. A. Werner and R. Pynn, J. Appl. Phys. **42**, 4736 (1971).
[9]G. Borelius, *The Changes in Energy Content, Volume, and Resistivity with Temperature in Simple Solids and Liquids*, Vol. 15 of *Solid State Physics*, edited by F. Seitz and D. Turnbull (Academic, New York, 1963), p. 1.
[10]C. M. McCarthy, C. W. Tompson, and S. A. Werner, Phys. Rev. B **22**, 574 (1980).
[11]A. A. Maradudin, E. W. Montroll, G. H. Weiss, and I. P. Ipatova, *Theory of Lattice Dynamics in the Harmonic Approximation*, 2nd ed. (Academic, New York, 1971), pp. 311–320.
[12]C. S. Barrett, Acta Crystallogr. **9**, 671 (1956).
[13]O. Balschko and G. Krexner, Phys. Rev. B **30**, 1667 (1984).
[14]A. A. Maradudin and P. A. Flinn, Phys. Rev. **129**, 2529 (1963).
[15]E. Aruja and H. Perlitz, Z. Krist. **100**, 195 (1938).